VISIBLE/NEAR-INFRARED SPECTRA OF CA-PYROXENE: EFFECTS OF Fe^{3+} AND SHOCK. M. C. McCanta[1] and M. D. Dyar[2], [1]Dept. of Earth & Planetary Sciences, University of Tennessee, 1412 Circle Dr, Knoxville TN 37909 (mmccanta@utk.edu), [2]Dept. of Astronomy, Mount Holyoke College, South Hadley MA 01075.

Introduction: Impact processes affect all bodies in the Solar System. Samples of planetary materials, including meteorites, lunar surface samples, and all potential returned surface samples from future exploration missions have the potential to be affected by impact. Because our current understanding of geologic processes on planetary bodies other than the Earth is based primarily on meteorite samples and lunar surface samples that have surely experienced impacts, determining the effects of impact-related thermal processes on redox ratio is of great importance in order to successfully interpret the magmatic history of these bodies.

Although impacts played a large role in delivering extraterrestrial samples to Earth for study, the extent to which shock processes affect the oxidation states of iron is unclear. Bauer [1] showed that impact-related thermal processes result in the oxidation of olivine in experimentally shocked samples. Minitti et al. [2] found the opposite trend in shocked hornblendes. Essene and Fisher [3] used thermodynamic calculations to show that reduction and volatization occur during high temperature events. Whether oxidizing or reducing, changes to the redox states of iron atoms that result from shock may mask the conditions that occurred in the source rock during its original crystallization. If redox ratio is used as a measure of the crystallization f_{O2} of a system, then shock processes may result in a compromised understanding of a planets' f_{O2} structure.

In this study, we examine effects of shock on pyroxene, a common meteorite constituent for which the redox ratio has been calibrated for use as an oxybarometer [4]. To determine if this oxybarometer records crystallization f_{O2} conditions or post-crystallization processes in shocked samples, effects of shock on pyroxene redox ratio must be understood. Additionally, we look at the effects that oxidation has on pyroxene spectral properties in the vis/NIR region to better comprehend remotely sensed data. The purpose of this study is thus to investigate the ability of impact-related thermal processes to change the redox signature of pyroxene and to constrain the effects of Fe^{3+} addition on pyroxene spectra.

Experimental and Analytical Methods: The target sample used in these experiments was a diopside from Jaipur, India ($Wo_{49}En_{48}Fs_3$). All shock experiments were encased in stainless steel (SS 304) containers. Projectiles were composed of polyethylene mounted with metal flyer plates of varying composition (stainless steel (SS 304), Fansteel 77, tungsten) determined by the desired shock pressure. Experiments were run over a range of shock pressures from 21 to 59 GPa. All experimental shocks took place under vacuum at relatively high p_{O2} conditions of ~10^{-4} atm with the exception of experiment number 3502. For this experiment, the impact chamber was first purged with N_2 gas to rid the system of excess oxygen and then a vacuum was applied prior to the shot. This created a lower f_{O2} environment than the previous shots with a p_{O2} of ~10^{-9} atm. Although f_{O2} was not directly measured or controlled in these experiments, this set-up allowed for lower p_{O2} conditions to be investigated.

Analytical methods. All shocked materials were analyzed for the major element compositions on the Johnson Space Center Cameca SX-100 electron microprobe. For Mössbauer analyses of Fe^{3+}, ~40 mg of unshocked and shocked pyroxenes from experimental runs were ground to a powder under acetone to prevent oxidation from the heat of grinding. Mössbauer spectra were acquired at 295K using a source of ~80 mCi ^{57}Co in Rh on a SEE Co. model WT302 spectrometer (Mount Holyoke College). Visible to near-infrared bidirectional reflectance spectra (0.3–2.6 μm, sampled at 5 nm increments) were acquired relative to halon at 30° incident, 0° emergent angles using the Reflectance Experiment Laboratory (RELAB) bidirectional spectrometer. The data were then corrected for the properties of halon. The same samples (in the same dish) were measured using a Pike diffuse reflectance attachment (off-axis, biconical) with the Thermo Nexus 870 FTIR spectrometer (2-50 μm, 5000-200 cm^{-1}) located at RELAB, using a diffuse gold standard.

Table 1. Redox States of Fe in Ca-Pyroxene

	P (GPa) (±3%)	% Fe^{3+} (±5%)	Target material
diopside	unshocked	9	particulate
3493	36	31	particulate
3494	43	24	particulate
3496	52	17	particulate
3495	59	27	particulate
3499	21	41	single crystal
3501	31	54	single crystal
3502	32	43	single crystal

Results: Shocked samples over the range of pressures studied exhibit both mechanical and chemical shock effects. TEM imaging suggests no evidence for the presence of submicron oxides or metal grains as observed in previous studies of olivine [i.e., 5,6]. Mössbauer data, however, show that all shocked samples are oxidized relative to the starting material (Table

1), although there is no clear trend with the amount of shock pressure.

The preferential oxidation of Fe^{2+} from the M2 sites is also seen in the reflectance spectra (Figure 1). With shock, there is a marked decrease in intensity of the band arising from Fe^{2+} in the M2 site at 2.0 μm. There is no commensurate increase in band intensity for Fe^{3+} features because they are such low intensity. As noted by many workers, i.e. [7], oxidized pyroxenes tend to have broad bands from spin-forbidden Fe^{3+} near 0.6 and 0.82 μm as well as $Fe^{2+}\leftrightarrow Fe^{3+}$ intervalence charge transfer bands near 0.8 μm. There is evidence for those bands in all our samples because they all contain Fe^{3+}, albeit in variable amounts. However, the Fe^{3+} bands are too weak to support any qualitative analyses.

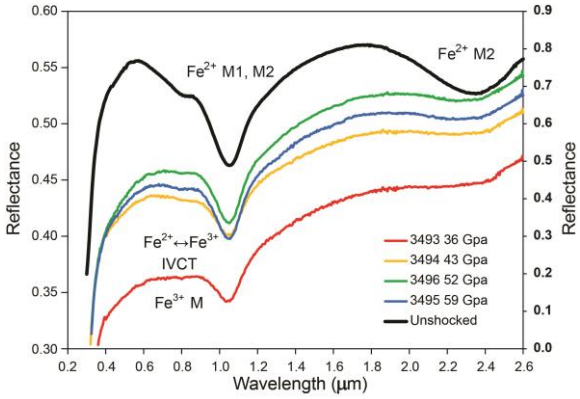

Figure 1. Vis/NIR reflectance data from the four particulate samples (left y axis) compared with the unshocked Jaipur diopside (right y axis). Single crystal experiments (#3499, #3501, and #3502) were not analyzed due to lack of sufficient sample mass.

Additionally, there is a strong decrease in the spectral slope between 400 and 600 nm in the shocked pyroxenes (Figure 2 top) [8]. This decrease is also observed in natural pyroxenes in SNC meteorites and in olivine, another mafic phase for which shock data is available. This change in slope does not appear to be related to increasing $Fe^{3+}/\Sigma Fe$ because highly oxidized Ca-pyroxenes from the terrestrial mantle display a distinct slope in this region (Figure 2 bottom).

Discussion: It is clear that the bulk chemistry of the pyroxene controls its crystal structure, and thus steric constraints may place limits the incorporation of Fe^{3+} into pyroxene as a function of composition, regardless of the shock the sample may have experienced. Orthopyroxene and low-Ca clinopyroxene rarely incorporate greater than 15% of the total Fe as Fe^{3+} in terrestrial occurrences, while higher Ca clinopyroxene can contain up to 50 - 60% Fe^{3+} [9] (Figure 2 bottom). Thus, we speculate that the unshocked diopside used here has the right composition to be oxidized by shock, and that orthopyroxenes and olivines might be

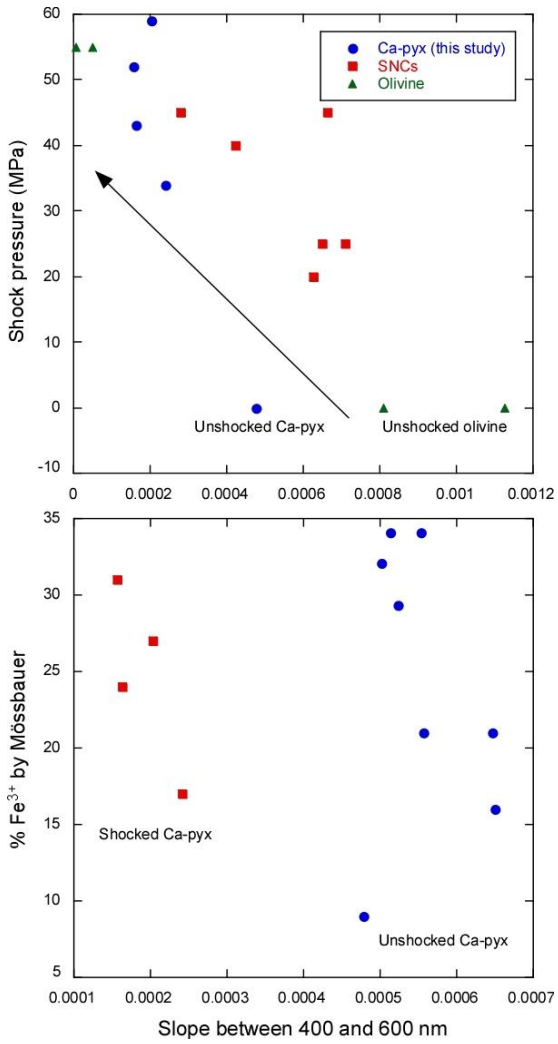

Figure 2. Change in slope between 400 and 600 nm as a function of (Top) shock pressure and (Bottom) $\%Fe^{3+}$. Unshocked, heavily oxidized Ca-pyx from Dish Hill, CA plotted for comparison.

less affected. Moreover, clinopyroxenes tend to contain more H to facilitate dehydrogenation [10,11] and provide a mechanism for shock oxidation.

References: [1] Bauer J. F. (1979) *Proc. 10th LPSC* 2573-2576. [2] Minitti M. E. et al. (2008) *EPSL, 266*, 288-302. [3] Essene E. J. and Fisher D. C. (1986) *Science*, 234, 189–193. [4] McCanta M. C. et al. (2004) *Amer. Mineral., 89*, 1685-1693. [5] Khisina N. R. et al. (1995) *Phys. Chem. Mins., 22*, 241-250. [6] Boland J. N. and Duba A. (1981) *Nature, 294*, 142-144. [7] Straub D. W. et al. (1991) *JGR, 96*, 18819-18830. [8] McCanta M. C. and Dyar M. D. (2016) *Met. Planet. Sci.*, doi: 10.1111/maps.12793. [9] Deer W. et al. (1978) Longman Group Limited, UK, 510 p. [10] Skogby H. et al. (1990) *Amer. Mineral. 75*, 764-774. [11] Smyth J. R. et al. (1991) *Nature, 351*, 732–735.